Asian Journal of Chemistry; Vol. 34, No. 9 (2022), 2444-2450

ASIAN JOURNAL OF CHEMISTRY

https://doi.org/10.14233/ajchem.2022.23893

Rhodium(III) and Platinum(II) Complexes of Azamacrocycle: Synthesis, Characterization and Antimicrobial Evaluation

SASWATA RABI[1], PRADIP PAUL[2], SAROJ K.S. HAZARI[3], BENU K. DEY[3], DEBASHIS PALIT[3], ISMAIL M.M. RAHMAN[4,*] and TAPASHI G. ROY[3,*]

[1]Department of Chemistry, Faculty of Engineering & Technology, Chittagong University of Engineering & Technology, Chattogram 4349, Bangladesh
[2]Department of Chemistry, Jashore University of Science and Technology, Jashore Sadar 7408, Bangladesh
[3]Department of Chemistry, Faculty of Science, University of Chittagong, Chattogram 4331, Bangladesh
[4]Institute of Environmental Radioactivity, Fukushima University, 1 Kanayagawa, Fukushima City, Fukushima 960-1296, Japan

*Corresponding authors: E-mail: immrahman@ipc.fukushima-u.ac.jp; tapashir57@cu.ac.bd

Received: 1 May 2022; *Accepted*: 28 July 2022; *Published online*: 19 August 2022; AJC-20945

A dihydroperchlorate salt of octamethyl derivative of 14-membered tetraazamacrocycle, Me_8[14]diene·2$HClO_4$ (L·2$HClO_4$), was formed by the condensation of 1,2-diamino propane with acetone in the presence of a quantitative amount of perchloric acid, which on extraction with chloroform at pH above 12 yielded free ligand (L). The interaction of rhodium(III) trichloride trihydrate and platinum(II) chloride with free ligand L produced six-coordinated octahedral orange-red complex, *cis*-[$RhLCl_2$]Cl and four-coordinated square-planar yellow complex, [PtL]Cl_2, respectively. Axial substitution reactions on [$RhLCl_2$]Cl with KX (X = NO_3, Br or I) and $NaNO_2$ afforded six-coordinated deep brown products [$RhLY_2$]Y (Y= NO_3, Br, I or NO_2). The ligand and metal complexes were characterized based on analytical, molar conductivity, spectroscopic and magnetochemical data. The antimicrobial activities of the concerned ligand and its complexes have been explored against some selected bacteria and fungi.

Keywords: Tetraazamacrocycle, Metal complexes, Axial substitution reactions, Antimicrobial activities.

INTRODUCTION

Research on macrocyclic ligands and their different metal complexes has been prioritized due to their diverse applications [1,2]. Macrocyclic compounds are playing a remarkable role in the pharmacological sector, such as in the remodeling of antibacterial [3], antifungal [4], antitumor [5] and anticancer [6] agents, and so forth. They are also useful as radioimmunotherapeutic [7] and MRI contrast [8] agents. *N*-pendent-armed macrocyclic complexes are considered in the development of medicinal chemistry [9-13]. Some metal complexes of 3,10-C-*meso*-Me_8[14]diene (L) and corresponding isomeric anes (L_A, L_B and L_C), as well as some *N*-pendent derivative ligands of these isomeric ligands and their metal complexes, have been studied [14-18].

We have also reported the synthesis and characterization of an octahedral diperchloratocopper(II) complex of Me_8[14]diene, [$CuL(ClO_4)_2$] and its axial substitution products [19,20]. However, free ligand L of octamethyl substituted tetraazamacrocyclic ligand salt Me_8[14]diene·2$HClO_4$ (L·2$HClO_4$) has not been comprehensively characterized [19]. Studies on Rh(III) with different macrocycles [21-28] have also been reported in the literature. Synthesis of platinum(II) complexes with macrocyclic ligands were also reported [22,23,29-32] and a few of them were with tetradentate tetraazamacrocyclic ligands [23,30,32]. So, it is interesting to carry out studies on rhodium(III) and platinum(II) complexes of Me_8[14]diene (L). Thus, systematic study on syntheses and characterization of octamethyl substituted tetraazamacrocyclic ligand (L), its rhodium(III) and platinum(II) complexes as well their antimicrobial studies are reported herein.

EXPERIMENTAL

All the chemicals used were of analytical reagent grade and used without further purification.

Physical measurements: Elemental analyses (C, H, N) were performed on a LECO CHNS-932 elemental analyzer (LECO Corporation, USA). NMR measurements (^{1}H, ^{13}C) were carried out on a Bruker AVANCE 400 spectrometer (Bruker AG, Germany). The chemical shifts were referenced to tetramethylsilane (TMS). Mass spectra were measured on a MAT 95XL Finnigan instrument (ThermoQuest Finnigan, Bremen, Germany) for electrospray ionization (ESI). UV-visible spectra were recorded on a Shimadzu UV-visible spectrophotometer (Shimadzu, Japan) in DMSO. Conductance measurements were carried out on a conductivity bridge HI-8820 (Hanna Instruments, Italy). Magnetic measurements were performed on Gouy Balance, which was calibrated using $Hg[Co(NCS)_4]$. IR spectra were recorded on a Shimadzu IR 20 spectrophotometer (Shimadzu, Japan) as KBr disks.

3,10-C-*meso*-Me_8[14]diene·2$HClO_4$ (L·2$HClO_4$): The ligand salt Me_8[14]diene·2$HClO_4$ (L·2$HClO_4$) was prepared by following the protocol as described by Bembi *et al.* [33].

Isolation of free ligand 3,10-C-*meso*-Me_8[14]diene (L): Isolation of free ligand has been performed following the protocol of Roy *et al.* [19]. Me_8[14]diene·2$HClO_4$ (20 g) was suspended in 100 mL of water. Sodium hydroxide was added to this solid to raise the mixture pH > 12 and excess NaOH addition was done to ensure that ligand was free from hydroperchlorate. The mixture was then heated on a water bath for 0.5 h. The free ligand was extracted with a 50 mL chloroform from the hot mix. The chloroform was then evaporated off, leaving behind a yellow oily liquid. On cooling, the oily liquid was solidified to a white product, Me_8[14]diene (L).

Free ligand L: Yield: 75% ($C_{18}H_{36}N_4$), (308.62); Colour: white; m.p.: 117 ºC. Anal. calcd. (found) %: C, 70.08 (70.12); H, 11.76 (11.71); N, 18.16 (18.12). IR (KBr disc, cm^{-1}): ν(N-H), 3165s; ν(C-H), 2960s; ν(CH_3), 1360s; ν(C-C), 1140vs; ν(C=N), 1660s. Mass (*m/z* value): Molecular ion peak, 308; Base peak, 98; Fragment peaks, 155, 139, 124, 85, 70, 41. ^{1}H NMR (400 MHz, DMSO, 25 ºC, TMS): For CH_3, δ = 1.500 (s, 6H, equatorial); 1.610 (ov, 12H, equatorial); For CH_2, CH & NH, δ = 2.160 (m), 2.890 (m), 3.570 (m), 3.880 (m), 4.470 (m). ^{13}C NMR (400 MHz, DMSO, 25 ºC, TMS): For peripheral carbon, 19.477, 19.947, 22.866, 24.518, 28.120, 28.826, 31.153, 32.768; For ring carbon, 48.095, 48.900, 49.557, 50.439, 50.510, 52.539, 52.627, 59.099 except for sp^2 carbons; For sp^2 carbon, 162.702, 171.950.

Rhodium(III) complex {*cis*-[$RhLCl_2$]Cl}: Rhodium(III) trichloride (0.264 g, 1.0 mmol) and free ligand L (0.308 g, 1.0 mmol) were separately dissolved in 20 mL hot methanol and the solutions were mixed. The resulting mixture was refluxed for 4 h. After that the reaction mixture was filtered and allowed to stand overnight while the deep orange-red product *cis*-[$RhLCl_2$]Cl was separated by filtration followed by washing with methanol and diethyl ether. Finally, the product was stored in a vacuum desiccator over silica gel. Yield: 64% Colour: deep orange red; m.p.: 225 ºC. Anal. calcd. (found) % for $C_{18}H_{36}N_4Cl_3Rh$ (*m.w.* 517.77): C, 41.75 (41.77); H, 7.01 (6.98); N, 10.82 (10.85). IR (KBr disc, cm^{-1}): ν(N-H), 3291s; ν(C-H), 2985s; ν(CH_3), 1365s; ν(C-C), 1140vs; ν(C=N), 1654s; ν(Rh-N), 500m. Molar conductivity: 72 ohm^{-1} cm^2 mol^{-1} in DMSO and 38 ohm^{-1} cm^2 mol^{-1} in DMF. ^{1}H NMR (400 MHz, DMSO, 25 ºC, TMS): For CH_3, δ = 1.847 (s, 6H, equatorial); 1.474 (ov, 18H, equatorial); For CH_2, CH & NH, δ = 2.055 (m), 7.765 (m), 6.946 (m), 7.263 (m), 8.576 (m). Magnetic moment μ_{eff} (B.M.): Diamagnetic. UV-vis [λ_{max} in nm (ε_{max})]: in DMSO, 364 (2161), 377 (3341), 380 (2183), 392 (2131).

Rhodium(III) complexes prepared by simultaneous axial substitution and anion exchange reactions on *cis*-[$RhLCl_2$]Cl:

***cis*-[$RhLX_m$]X_n (X = NO_3, Br, I or NO_2; m = 2 or 1; n = 1 or 2):** *cis*-[$RhLCl_2$]Cl (0.517 g, 0.1 mmol) and KY (3.0 mmol; Y = NO_3, Br or I) or $NaNO_2$ (3.0 mmol) were suspended separately in 25 mL hot methanol and then mixed. After mixing, the orange-red colour of the supernatant liquids turned light brown within a few minutes. Then the resulting mixtures after 4 h reflux were filtered and allowed to stand overnight. Later, deep brown products *cis*-[$RhL(NO_3)](NO_3)_2$, *cis*-[$RhLBr_2$]Br, *cis*-[$RhLI_2$]I and *cis*-[$RhL(NO_2)_2](NO_2)$ were separated, respectively, by filtration followed by washing with methanol and diethyl ether. Finally, the products were stored in a vacuum desiccator over silica gel.

***cis*-[$RhL(NO_3)](NO_3)_2$**: Yield: 58%; colour: deep brown; m.p.: 205 ºC. Anal. calcd. (found) % for $C_{18}H_{36}N_7O_9Rh$ (*m.w.* 597.42): C, 36.19 (36.22); H, 6.07 (6.04); N, 16.41 (16.43). IR (KBr disc, cm^{-1}): ν(N-H), 3190s; ν(C-H), 2980s; ν(CH_3), 1383m; ν(C-C), 1144s; ν(C=N), 1658s; ν(Rh-N), 502m; ν(NO_3), 1460 m, 1280sh, ν_2 = 834m, ν_3 = 1390w, ν_4 = 715m. Molar conductivity: 166 ohm^{-1} cm^2 mol^{-1} in DMSO and 35 ohm^{-1} cm^2 mol^{-1} in DMF. Magnetic moment μ_{eff} (B.M.): Diamagnetic. UV-vis [λ_{max} in nm (ε_{max})]: in DMSO, 372 (1621), 391 (1627), 401 (1594).

***cis*-[$RhLBr_2$]Br**: Yield: 64%; Colour: deep brown; m.p.: 218 ºC. Anal. calcd. (found) % for $C_{18}H_{36}N_4Br_3Rh$ (*m.w.* 651.12): C, 33.20 (33.26); H, 5.57 (5.59); N, 8.60 (8.57). IR (KBr disc, cm^{-1}): ν(N-H), 3283s; ν(C-H), 2995w; ν(CH_3), 1350w; ν(C-C), 1145s; ν(C=N), 1658s; ν(Rh-N), 501m. Molar conductivity: 85 ohm^{-1} cm^2 mol^{-1} in DMSO and 36 ohm^{-1} cm^2 mol^{-1} in DMF. Magnetic moment μ_{eff} (B.M.): Diamagnetic. UV-vis [λ_{max} in nm (ε_{max})]: in DMSO, 295 (4000), 376 (2557), 382 (2544). ^{1}H NMR (400 MHz, DMSO, 25 ºC, TMS): For CH_3, δ = 2.054 (s, 6H, equatorial); 2.483 (ov, 18H, equatorial); For CH_2, CH & NH, δ = 2.639, 6.764 (m), 6.946 (m), 7.263 (m), 8.577 (m).

***cis*-[$RhLI_2$]I:** Yield: 57%; Colour: deep brown; m.p.: 208 ºC. Anal. calcd. (found) % for $C_{18}H_{36}N_4I_3Rh$ (*m.w.* 792.12): C, 27.29 (27.31); H, 4.58 (4.60); N, 7.07 (7.02). IR (KBr disc, cm^{-1}): ν(N-H), 3282s; ν(C-H), 2990w; ν(CH_3), 1362w; ν(C-C), 1145s; ν(C=N), 1657s; ν(Rh-N), 502m. Molar conductivity: 91 ohm^{-1} cm^2 mol^{-1} in DMSO and 39 ohm^{-1} cm^2 mol^{-1} in DMF. Magnetic moment μ_{eff} (B.M.): Diamagnetic. UV-vis [λ_{max} in nm (ε_{max})]: in DMSO, 298 (2113), 382 (1444), 394 (1436).

***cis*-[$RhL(NO_2)_2](NO_2)$:** Yield: 67%; Colour: deep brown; m.p.: 212 ºC. Anal. calcd. (found) % for $C_{18}H_{36}N_7O_6Rh$ (*m.w.* 549.43): C, 39.35 (39.38); H, 6.60 (6.58); N, 17.85 (17.81). IR (KBr disc, cm^{-1}): ν(N-H), 3245s; ν(C-H), 2995w; ν(CH_3), 1383w; ν(C-C), 1144s; ν(C=N), 1657s; ν(Rh-N), 502m; $\nu(NO_2)_{asym}$, 1473s, $\nu(NO_2)_{sym}$ 1350m, δ_{NO_2} 828s, ν(NO_2-), 1270s, 1325w. Molar conductivity 69 ohm^{-1} cm^2 mol^{-1} in DMSO and

40 ohm^{-1} cm^2 mol^{-1} in DMF. Magnetic moment μ_{eff} (B.M.): Diamagnetic. UV-vis [λ_{max} in nm (ε_{max})]: in DMSO, 373 (946), 386 (940), 391 (923).

Platinum(II) complex [PtL]Cl_2: Platinum(II) dichloride (0.265 g, 1.0 mmol) and free ligand L (0.308 g, 1.0 mmol) were dissolved separately in 20 mL hot ethanol and then mixed. The resulting mixture was refluxed for 12 h. Within a few hours, the orange-red solution turned to cream colour slowly. Then the reaction mixture was allowed to stand overnight while the yellow product of [PtL]Cl_2 was separated by filtration, followed by washing with ethanol and diethyl ether. Finally, the product was stored in a vacuum desiccator over silica gel.

[PtL]Cl_2: Yield: 62%; colour: yellow. m.p.: 228 ºC. Anal. calcd. (found) % for $C_{18}H_{36}N_4Cl_2Pt$ (*m.w*. 574.49): C, 37.63 (37.66); H, 6.32 (6.31); N, 9.75 (9.78). IR (KBr disc, cm^{-1}): ν(N-H), 3270s; ν(C-H), 2985w; ν(CH_3), 1384w; ν(C-C), 1133s; ν(C=N), 1650s; ν(Pt-N), 437m. Molar conductivity: 166 ohm^{-1} cm^2 mol^{-1} in DMSO. ^{1}H NMR (400 MHz, DMSO, 25 ºC, TMS): For CH_3, δ = 1.178 (s, 6H, equatorial), 1.255 (s, 6H, axial), 1.183 (s, 3H, equatorial) 1.892 (s, 3H, equatorial), 2.053 (s, 3H, equatorial); For CH_2 & NH, δ = 1.312 (s, 2H), 1.395 (s, 2H), 2.636 (m), 2.604 (m), 2.958 (m), 4.082 (m), 6.300 (m), 8.705 (m), 9.600 (m). ^{13}C NMR (400 MHz, DMSO, 25 ºC, TMS): For peripheral carbon, 16.14, 16.36, 18.76, 19.02, 20.34, 24.42, 24.68, 31.19; For ring carbon, 42.98, 46.51, 51.98, 52.38, 52.53, 55.82, 56.05, 57.92 except for sp^2 carbons; For sp^2 carbon, 173.6. Magnetic moment μ_{eff} (B.M.): Diamagnetic. UV-vis [λ_{max} in nm (ε_{max})]: in DMSO, 261 (1198), 357 (126), 362 (45), 375 (20), 411 (20).

Antibacterial activities: Antibacterial activities of the ligand and its Rh(III) and Pt(II) complexes against selected Gram-positive and Gram-negative bacteria were investigated by the disc diffusion method. Paper disc (6 mm in diameter) and Petri plates (70 mm in diameter) were used throughout the experiment. Pour plates were made with sterilized melted nutrient agar (45 ºC). After solidification of nutrient agar, the test organisms (suspension in sterilized water) were spread uniformly over the nutrient agar with sterilized glass rods separately. After soaking with test chemicals (1 mg/1 mL in DMSO), the paper discs were placed at the center of the inoculated pour plates. A control plate was also maintained in each case with DMSO. At first, the plates were left for 4 h at a low temperature (4 ºC) and the test chemicals diffused from disc to the surrounding medium by this time. The plates were then incubated at 35 ± 2 ºC for growth of test organisms and were observed at 24 and 48 h intervals. The activity was expressed in terms of the zone of inhibition in mm. The results for all concerned compounds have been reported after subtracting values for solvent DMSO itself. Tests were performed in triplicates for statistical analysis.

Antifungal activities: The poisoned food technique was used to assess the *in vitro* antifungal activities of the ligand and its complexes against selected phytopathogenic fungi. Potato dextrose agar (PDA) was used as a growth medium. DMSO was used as the solvent to prepare solutions of the tested compounds. The solutions were then mixed with the sterilized PDA to maintain concentrations of the compounds of 1% solution (mg/mL). 20 mL of these solutions were each poured into a petri dish. After solidifying the medium, a 5 mm mycelial disc of each fungus was placed in the center of each assay plate, along with a control. Linear growth of the fungus was measured in mm after five days of incubation at 25 ± 2 ºC.

RESULTS AND DISCUSSION

Free ligand 3,10-C-*meso*-Me_8[14]diene (L): The infrared spectrum of this free ligand exhibits ν(N–H), ν(C–H), ν(CH_3), ν(C–C) and ν(C=N) bands at 3165 cm^{-1}, 2960 cm^{-1}, 1380 cm^{-1}, 1141 cm^{-1} and 1660 cm^{-1}, respectively. However, the absence of bands at around 1100 cm^{-1} and 620 cm^{-1} indicate that no ClO_4^- group is present in this ligand, *i.e.* L is a free ligand other than dihydroperchlorate salt. The mass spectrum of this macrocyclic ligand L shows *m/e* at 308 due to molecular ion peak and base peak at *m/z* value 98 due to a stable fragment. This spectrum also exhibits several peaks at *m/z* values 155, 139, 124, 98, 85, 70 and 41, corresponding to different fragments. The fragmentation pattern of this compound is a piece of evidence in support of the structural formula of L. ^{1}H NMR spectrum displays a sharp methyl singlet at 1.500 ppm corresponding to 6H and an unresolved multiplet at 1.610 ppm corresponding to 18H. The singlet at 1.500 ppm can be assigned to a pair of equatorial methyl protons of *gem*-dimethyl groups. The other singlet for a pair of methyls of *gem*-dimethyl that is expected to appear at a position downfield in comparison overlaps with singlet corresponding to imine methyls at C_5 and C_{12} and doublets arising out of methyls at C_3 and C_{10} positions. The pattern suggests an entirely symmetrical C-*meso* structure of L (**Scheme-I**), in which imine methyls at C_5 and C_{12} and chiral methyls at C_3 and C_{10} positions are all equatorial. A similar assignment has been made for nickel(II) complexes [34]. All the chiral methyls have an equatorial orientation in this ligand. It has been concluded that ligand shows only one methyl singlet for *gem* dimethyl group along with an unresolved signal must be *meso*-diastereoisomer or racemic diastereoisomer [34]. A completely *meso*-configuration is assigned for L (**Scheme-I**) with all chiral and imine methyls equatorial. The spectrum further explores the appearance of five multiplets at 2.160, 2.890, 3.570, 3.880 and 4.470 ppm due to methylene, methine and amine protons.

The number of signals observed in its ^{13}C NMR spectrum corresponds to a number of non-equivalent carbon atoms. Assignments are made on a literature basis [14-17]. Based on the ^{1}H NMR spectral analysis, although the ligand seems to be a symmetrical one with all equatorial orientation, the appearance of a separate signal for each carbon can be accounted for the distortion in the structure. The eight peaks in the range of 15-30 ppm have been assigned for eight peripheral carbons and other eight in the range of 40-65 ppm for ring carbons except for sp^2 carbons. In this case, peaks at 167 and 171 ppm have been assigned for two sp^2 carbons. Thus, ligand L exhibits 18 peaks for 18 non-equivalent carbons. So, all these analytical data are in favour of the structure of free ligand L.

Metal complexes of free diene ligand L

Rhodium(III) complexes, *cis*-[RhLZ_m]Z_n (Z= Cl, NO_3, Br, I or NO_2; m = 2 or 1; n = 1 or 2): Interaction between

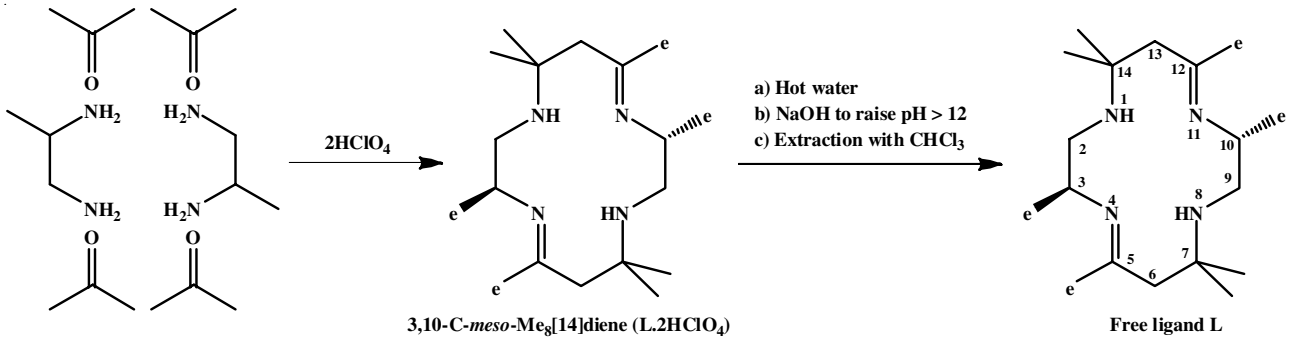

Scheme-I: Preparation of ligand

rhodium(III) trichloride and free ligand L in a methanolic solution on 4 h of reflux afforded six-coordinated octahedral orange-red complex *cis*-$[RhLCl_2]Cl$, while *cis*-$[RhLCl_2]Cl$ underwent simultaneous axial substitution and anion exchange reactions with KNO_3, $NaNO_2$, KBr and KI in the ratio of 1:3 to yield brown axial substitution and anion exchange products, *cis*-$[RhL(NO_3)](NO_3)_2$, *cis*-$[RhL(NO_2)_2](NO_2)$, *cis*-$[RhLBr_2]Br$ and *cis*-$[RhLI_2]I$, respectively. The infrared spectra of these complexes display ν(N–H), ν(C–H), ν(C–C), ν(C=N) and ν(CH_3) bands at 3291-3245 cm^{-1}, 2995-2980 cm^{-1}, 1145-1133 cm^{-1}, 1654-1617 cm^{-1} and 1383-1350 cm^{-1}, respectively. Further, ν(Rh–N) band at 502-500 cm^{-1} in these spectra support the formation of *cis*-complexes [23,26]. Multiplicity of bands from 800 to 900 cm^{-1} also supports the formation of *cis* complexes [23,26,27]. The spectrum of *cis*-$[RhL(NO_3)](NO_3)_2$ further exhibits bands at 1460 cm^{-1} and 1280 cm^{-1} attributed to the coordinated NO_3^- group and the separation of these bands by 180 cm^{-1} is accounted for a bidentate mode of coordination [35]. This spectrum also reveals bands at 834, 1390 and 720 cm^{-1} due to ionic NO_3^- group [35,36]. Similarly, the complex *cis*-$[RhL(NO_2)_2](NO_2)$ displays the $\nu_{asym}(NO_2)$ and $\nu_{sym}(NO_2)$ bands at 1473 and 1350 cm^{-1}, respectively. The appearance of band at 828 cm^{-1} can be attributed to δ_{NO_2} frequency. This spectrum also exhibits bands at 1270 and 1325 cm^{-1} due to the ionic NO_2^- group. It is to be observed that band at 611 cm^{-1} supports complex *cis*-$[RhL(NO_2)_2](NO_2)$ to be N-bonded nitro complex [35,36]. Since IR spectra could not be run at a range lower than 400 cm^{-1}, the bands below 400 cm^{-1} due to Rh-Cl/Br/I could not be recorded. The molar conductivity values 69-91 ohm^{-1} cm^2 mol^{-1} in DMSO for all *cis*-Rh(III) complexes except *cis*-$[RhL(NO_3)](NO_3)_2$ correspond almost to 1:1 electrolytes. But the molar conductivity value 166 ohm^{-1} cm^2 mol^{-1} in DMSO of *cis*-$[RhL(NO_3)](NO_3)_2$ corresponds to 1:2 electrolytes as expected for the molecular formula assigned. However, the molar conductivity values 35-38 ohm^{-1} cm^2 mol^{-1} in DMF for each *cis* rhodium(III) complex indicate the incorporation of Z^- in the coordination sphere, which should increase the coordination number of Rh(III) from 6 to 7, but practically anion association in the coordination sphere occurs as observed in our earlier studies [15]. The electronic spectra of these complexes exhibit bands at 357-411 nm in DMSO, supporting the formation of six-coordinated octahedral rhodium(III) complexes [23,26,27]. In case of octahedral rhodium(III) complexes, two spin-allowed transitions $^1A_{1g} \rightarrow {}^1T_{1g}$ and $^1A_{1g} \rightarrow {}^1T_{2g}$ can occur [23,26,27]. However, the larger extinction coefficient values of this complex support the formation of *cis* complex [26]. The electronic spectra also display charge transfer bands at 261-298 nm. ^{1}H NMR spectrum of *cis*-$[RhLCl_2]Cl$ explores one singlet at 1.847 ppm corresponding to 6H, which originates from the equatorial components of two *gem*-dimethyl pairs. The spectrum further shows an overlapped signal at 2.474 ppm resolved for one doublet and two singlets, among which the doublet corresponding to 6H can be assigned to equatorially oriented two methyl protons on two chiral carbons and one singlet corresponding to 6H can be attributed to axial components of *gem*-dimethyl groups and the other singlet corresponding to 6H can be accounted for equatorially oriented two methyl protons on sp^2 carbons. The further appearance of downfield multiplets at 2.054, 6.765, 6.946, 7.263 and 8.576 ppm can be accounted for CH_2, CH and NH protons. Thus, an all-equatorially oriented structure (str. 1 in Fig. 1) can be assigned for this complex. Similarly, the ^{1}H NMR spectrum of *cis*-$[RhLBr_2]Br$ exhibits one singlet at 2.054 ppm (6H) for equatorial components of two *gem*-dimethyl pairs and an overlapped signal at 2.483 ppm, which can be resolved for two singlets and one doublet as observed for mother complex *cis*-$[RhLCl_2]Cl$. So, the same assignment can be made for this complex too. It gives evidence that since this complex has been synthesized by axial substitution reaction on mother complex *cis*-$[RhLCl_2]Cl$, the stereochemistry of ligand of this complex should be the same as ligand of mother complex, considering that axial addition and substitution reactions take place without change of configuration and conformation of the ligand of original complexes [16-19]. The further appearance of downfield multiplets at 2.639, 6.765, 6.946, 7.263 and 8.576 ppm are due to CH_2, CH and NH protons. Thus, an all-equatorially oriented structure (str. 3 in Fig. 1) can also be assigned for this complex. Based on all these evidences, str. 1 to 5 (Fig. 1) can be assigned for *cis*-rhodium(III) complexes, *cis*-$[RhLCl_2]Cl$, *cis*-$[RhL(NO_3)](NO_3)_2$, *cis*-$[RhLBr_2]Br$, *cis*-$[RhLI_2]I$ and *cis*-$[RhL\text{-}(NO_2)_2](NO_2)$, respectively.

Platinum(II) complex: The reaction between the free ligand L and platinic chloride in the ratio of 1:1 resulted in a yellow product, $[PtL]Cl_2$. The infrared spectrum of this complex reveals bands at 3270 and 1650 cm^{-1} due to ν(N–H) and ν(C=N), respectively. Additional bands for ν(C–H), ν(CH_3) and ν(C–C) are also observed in the expected regions. The band for Pt-Cl expected at around 260 cm^{-1} could not be detected as the spectrum could not be run below 400 cm^{-1}. Further, the

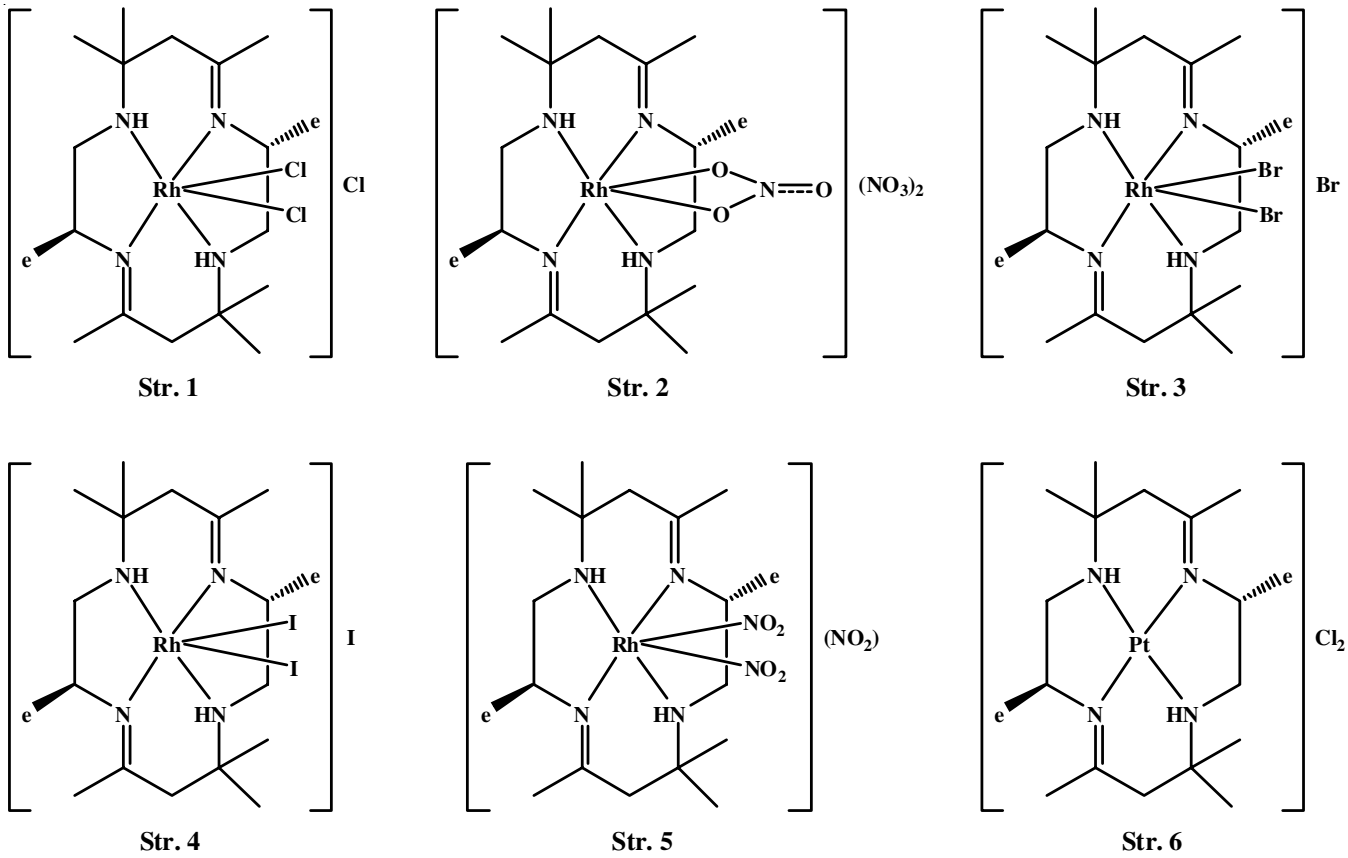

Fig. 1. Rhodium(III) and platinum(II) complexes of free ligand L

spectrum exhibits ν(Pt–N) band at 437 cm^{-1} as observed in the literature [30,31]. The molar conductivity of 166 ohm^{-1} cm^2 mol^{-1} in DMSO indicates that this complex is 1:2 electrolyte as expected [30,31]. The electronic spectrum of this complex exhibits bands at 337-375 nm in DMSO, which support the formation of four-coordinated square-planar platinum(II) complex [23,31,37] and reasonably assigned to $^1A_{1g} \rightarrow {}^1B_{1g}$ and $^1A_{1g} \rightarrow {}^1E_g$ transition [23,31,37]. However, the appearance of *d–d* transition at 411 nm can be assigned to $^1A_{1g} \rightarrow {}^1A_{2g}$ transition [23]. The spectrum also exhibits a charge transfer band at 261 nm. The ^{1}H NMR spectrum of this complex explores six singlets and one doublet. Two singlets at 1.178 and 1.255 ppm each corresponding to 6H can be assigned to equatorial and axial components of *gem*-dimethyl protons, respectively. However, the only doublet at 1.183 ppm corresponding to 6H can be attributed to two equatorially oriented methyls on C_3 and C_{10} chiral carbons. Again, two singlets at 1.312 and 1.395 ppm each corresponding to 2H can be accounted for β-methylene protons on C_6 and C_{13} carbons. Moreover, the singlets at 1.892 and 2.053 ppm, each corresponding to 3H, can be assigned to two equatorially oriented methyl protons on two sp^2 carbons. The further appearance of downfield multiplets at 2.367, 2.604, 2.958, 4.082, 6.300, 8.705 and 9.600 ppm may be due to CH_2, CH and NH protons. Thus, an all-equatorially oriented structure (str. 6 in Fig. 1) can be assigned for this complex. However, the ^{13}C NMR spectrum of $[PtL]Cl_2$ reveals 17 peaks: 8 peaks in the range of 16 to 31 ppm for eight peripheral carbons and eight peaks at 43 to 58 ppm for eight ring carbons (except for two sp^2 carbons). The spectrum also displays one peak at 173.62 ppm due to two equivalent sp^2 carbons. This assignment is in support of distortion in the molecule. Thus, the molecular structure of $[PtL]Cl_2$ can be assigned as str. 6 (Fig. 1).

Antibacterial activities: Due to the pharmacological importance, investigation of the antibacterial activities of the concerned macrocyclic ligand and its metal [Rh(III) and Pt(II)] complexes, non-coordinated metal salts, solvent DMSO (as control) and standard antibacterial agent have been carried out against Gram-positive bacteria (*Staphylococcus aureus, Bacillus cereus* and *Bacillus subtilis*) and Gram-negative bacteria (*Pseudomon asaeruginosa, Salmonella typhi* and *Escherichia coli*) (Table-1). In this study, different compounds showed various extent of activity against the bacteria. The macrocyclic ligand L does not show any activity, as observed in some earlier studies [16-21]. On the other hand, platinum(II) dichloride complex (S6, Table-1) against all Gram-positive bacteria and dichloridorhodium(III) chloride complex (S1, Table-1) against all Gram-negative bacteria showed the highest activity among the concerned complexes. Other than these two complexes, S2 and S4 also exhibit high potentiality against all Gram-positive bacteria, whereas S3 and S5 show moderate activity against all bacteria except for S3 against one Gram-negative bacteria. Though the metal salt $PtCl_2$ is itself poisonous, the stability of the complex with Pt(II) (very much stable in solutions also) prevents the liberation of ligand or metal ion in the test media [38]. Thus, the activity observed for the Pt(II) complex is not due to free Pt(II) ion.

TABLE-1
ANTIBACTERIAL ACTIVITY AGAINST GRAM-POSITIVE BACTERIA

Sample code	Test compounds	Diameter of zone of inhibition (mm); 24 h incubation					
		Gram-positive			Gram-negative		
		S. aureus	*B. cereus*	*B. subtilis*	*S. typhi*	*P. asaeruginosa*	*E. coli*
L1	L (Free)	0	0	0	0	0	0
S1	*cis*-[$RhLCl_2$]Cl	0	8	11	28	23	20
S2	*cis*-[$RhL(NO_3)$]$(NO_3)_2$	15	10	11	8	8	7
S3	*cis*-[$RhL(NO_2)_2$](NO_2)	7	11	8	0	10	12
S4	*cis*- [$RhLBr_2$]Br	15	18	21	0	0	0
S5	*cis*- [$RhLI_2$]I	10	12	12	11	12	13
S6	[PtL]Cl_2	26	28	20	10	7	0
S7	$RhCl_3 \cdot 3H_2O$	2	0	4	0	3	3
M1	$PtCl_2$	10	11	11	12	10	12
Control	DMSO	0	0	0	0	0	0
Standard	Ampicillin	26	25	23	26	27	24

TABLE-2
ANTIFUNGAL ACTIVITIES AGAINST DIFFERENT FUNGI

Sample code	Test compounds	% of inhibition of mycelial growth			
		S. niger	*F. equiseti*	*Penicillium*	*A. flavus*
L1	L (Free)	10	40	25	23
S1	*cis*-[$RhLCl_2$]Cl	42	100	100	33
S2	*cis*-[$RhL(NO_3)$]$(NO_3)_2$	100	100	85	100
S3	*cis*-[$RhL(NO_2)_2$](NO_2)	100	23	65	100
S4	*cis*-[$RhLBr_2$]Br	42	38	81	46
S5	*cis*-[$RhLI_2$]I	14	100	100	55
S6	[PtL]Cl_2	55	84	100	56
M1	$RhCl_3.3H_2O$	0	0	0	0
M2	$PtCl_2$	52	55	61	55
Control	DMSO	0	0	0	0
Standard	Griseofulvin	54	45	62	64

Antifungal activities: The antifungal activities are also interesting to determine the macrocyclic compounds' biological activities. Thus, the *in vitro* evaluation of antifungal activities of the concerned ligand, its different Rh(III) and Pt(II) complexes, non-coordinated metal salts and standard fungicide, griseofulvin, have been studied. Four fungi, *Aspergillus niger*, *Fusarium equiseti*, *Penicillium* and *Aspergillus flavus* have been used in this study. From the results, as summarized in Table-2, it is evident that almost all Rh(III) and Pt(II) complexes are sensitive to all the four fungal phytopathogens and it is interesting to note that a good number of tested compounds showed 100% inhibition against some fungi. Some of these complexes are more sensitive than standard griseofulvin against all phytopathogens. It is also to be observed that some of the compounds show higher activity even 100% (*e.g.*, S1 and S5 against *F. equiseti* and *Penicillium*, S2 against *S. niger*, *F. equsiti* and *A. flavus*, S3 against *S. niger* and *A. flavus*, S6 against *Penicillium*). These Rh(III) and Pt(II) complexes possess the highest potentiality as antifungal agents in this study.

Conclusion

Ligand salt 3,10-C-*meso*-Me_8[14]diene·2$HClO_4$(L·2$HClO_4$) on extraction with chloroform at pH above 12 yielded free diene ligand Me_8[14]diene (L). Rhodium(III) chloride on interaction with L resulted in octahedral rhodium(III) complex with *cis*-configuration, which underwent the simultaneous axial substitution and anion exchange reactions with K and Na salts to furnish different octahedral derivative complexes with the same configuration. Similarly, the free ligand on reaction with platinum(II) chloride afforded the square-planar platinum(II) complex. All the complexes exhibited excellent antibacterial and antifungal activities against selected bacteria and fungi.

ACKNOWLEDGEMENTS

The study was supported by grants from Ministry of Education, People's Republic of Bangladesh (PS2017552), Environmental Radioactivity Research Network Center at Fukushima University, Japan (I-22-11) and Grants-in-Aid for Scientific Research (21K12287) from the Japan Society for the Promotion of Science (JSPS).

CONFLICT OF INTEREST

The authors declare that there is no conflict of interests regarding the publication of this article.

REFERENCES

1. I.M. Kolthoff, *Anal. Chem.*, **51**, 1 (1979); https://doi.org/10.1021/ac50041a001
2. N.S. Al-Radadi, S.M. Al-Ashqar and M.M. Mostafa, *J. Incl. Phenom. Macro.*, **69**, 157 (2011); https://doi.org/10.1007/s10847-010-9826-0
3. A. Chaudhary, N. Bansal, A. Gajraj and R.V. Singh, *J. Inorg. Biochem.*, **96**, 393 (2003); https://doi.org/10.1016/S0162-0134(03)00157-0

4. N. Raman, J. Joseph, A.S.K. Velan and C. Pothiraj, *Mycobiology*, **34**, 214 (2006); https://doi.org/10.4489/MYCO.2006.34.4.214
5. D.S. Lamani, S.G. Badiger, K.R.V. Reddy and H.S.B. Naik, *Nucleos. Nucleot. Nucl.*, **37**, 498 (2018); https://doi.org/10.1080/15257770.2018.1498515
6. S. Ali, V. Singh, P. Jain and V. Tripathi, *J. Saudi Chem. Soc.*, **23**, 52 (2019); https://doi.org/10.1016/j.jscs.2018.04.005
7. P.V. Bernhardt and P.C. Sharpe, *Inorg. Chem.*, **39**, 4123 (2000); https://doi.org/10.1021/ic000315f
8. K. Xu, N. Xu, B. Zhang, W. Tang, Y. Ding and A. Hu, *Dalton Trans.*, **49**, 8927 (2020); https://doi.org/10.1039/D0DT00248H
9. M. Vicente, R. Bastida, C. Lodeiro, A. Macías, A.J. Parola, L. Valencia and S.E. Spey, *Inorg. Chem.*, **42**, 6768 (2003); https://doi.org/10.1021/ic034245z
10. N. Nishat and M.M. Haq, *Synth. React. Inorg. Met.-Org. Chem.*, **34**, 335 (2004); https://doi.org/10.1081/SIM-120028305
11. T.G. Roy, S.K.S. Hazari, B. Dey, B.C. Nath, A. Dutta, F. Olbrich and D. Rehder, *Inorg. Chim. Acta*, **371**, 63 (2011); https://doi.org/10.1016/j.ica.2011.03.011
12. T.G. Roy, S.K.S. Hazari, B.K. Dey, A. Nath, D.I. Kim, E.H. Kim and Y.C. Park, *J. Incl. Phenom. Macrocycl. Chem.*, **58**, 249 (2007); https://doi.org/10.1007/s10847-006-9150-x
13. M. Shakir, Y. Azim, H.T.N. Chishti, N. Begum, P. Chingsubam and M.Y. Siddiqi, *J. Braz. Chem. Soc.*, **17**, 272 (2006); https://doi.org/10.1590/S0103-50532006000200009
14. F.B. Biswas, S. Rabi, K. Barua, T.G. Roy, D. Palit and B.K. Dey, *Eur. Sci. J.*, **14**, 330 (2018); https://doi.org/10.19044/esj.2018.v14n24p330
15. T.G. Roy, S.K.S. Hazari, K.K. Barua, D.I. Kim, Y.C. Park and E.R.T. Tiekink, *Appl. Organomet. Chem.*, **22**, 637 (2008); https://doi.org/10.1002/aoc.1451
16. T.G. Roy, S.K.S. Hazari, B.K. Dey, H.A. Miah, F. Olbrich and D. Rehder, *Inorg. Chem.*, **46**, 5372 (2007); https://doi.org/10.1021/ic061700t
17. T.G. Roy, S.K.S. Hazari, H.A. Miah, S.K.D. Gupta, P.G. Roy, U. Behrens and D. Rehder, *Inorg. Chim. Acta*, **415**, 124 (2014); https://doi.org/10.1016/j.ica.2014.02.041
18. M.S. Alam, S. Rabi, M.M. Rahman, A. Baidya, M. Debi and T.G. Roy, *J. Chem. Sci.*, **130**, 35 (2018); https://doi.org/10.1007/s12039-018-1438-z
19. T.G. Roy, S.K.S. Hazari, B.K. Dey, S. Chakraborti and E.R.T. Tiekink, *Met. Based Drugs*, **6**, 345 (1999); https://doi.org/10.1155/MBD.1999.345
20. S.K.S. Hazari, T.G. Roy, B.K. Dey, S. Chakrabarti and E.R.T. Tiekink, *Z. Krist-New Cryst. St.*, **214**, 51 (1999); https://doi.org/10.1515/ncrs-1999-0129
21. T.M. Hood, M.R. Gyton and A.B. Chaplin, *Dalton Trans.*, **49**, 2077 (2020); https://doi.org/10.1039/C9DT04474D
22. S. Chandra, M. Tyagi and S. Agrawal, *J. Saudi Chem. Soc.*, **15**, 49 (2011); https://doi.org/10.1016/j.jscs.2010.09.005
23. M. Shakir, O.S.M. Nasman, A.K. Mohamed and S.P. Varkey, *Synth. React. Inorg. Met.-Org. Chem.*, **25**, 1671 (1995); https://doi.org/10.1080/15533179508014690
24. S.J. Swamy, B.V. Pratap, P. Someshwar, K. Suresh and D. Nagaraju, *J. Chem. Res.*, **2005**, 313 (2005); https://doi.org/10.3184/0308234054323986
25. T.M. Hood, B. Leforestier, M.R. Gyton and A.B. Chaplin, *Inorg. Chem.*, **58**, 7593 (2019); https://doi.org/10.1021/acs.inorgchem.9b00957
26. E.J. Bounsall and S.R. Koprich, *Can. J. Chem.*, **48**, 1481 (1970); https://doi.org/10.1139/v70-243
27. P.K. Bhattacharya, *J. Chem. Soc. Dalton*, 810 (1980); https://doi.org/10.1039/dt9800000810
28. A. Dei and L. Pardi, *Inorg. Chim. Acta*, **181**, 3 (1991); https://doi.org/10.1016/S0020-1693(00)85251-2
29. G.J. Grant, D.F. Galas, M.W. Jones, K.D. Loveday, W.T. Pennington, G.L. Schimek, C.T. Eagle and D.G. VanDerveer, *Inorg. Chem.*, **37**, 5299 (1998); https://doi.org/10.1021/ic9715714
30. M. Tyagi, S. Chandra and S.K. Choudhary, *J. Chem. Pharm. Res.*, **3**, 56 (2011).
31. S. Rani, S. Kumar and S. Chandra, *Synth. React. Inorg. Met.-Org. Nano-Met. Chem.*, **40**, 940 (2010); https://doi.org/10.1080/15533174.2010.522663
32. A.E.-M.M. Ramadan and T.I. El-Emary, *Transition Met. Chem.*, **23**, 491 (1998); https://doi.org/10.1023/A:1006988529965
33. R. Bembi, S. M. Sondhi, A. K. Singh, A. K. Jhanji, T. G. Roy, J.W. Lown and R.G. Ball, *Bull. Chem. Soc. Jpn.*, **62**, 3701 (1989); https://doi.org/10.1246/bcsj.62.3701
34. L.G. Warner and D.H. Busch, *J. Am. Chem. Soc.*, **91**, 4092 (1969); https://doi.org/10.1021/ja01043a014
35. K. Nakamoto, Infrared and Raman Spectra of Inorganic and Coordination Compounds, Wiley: Hoboken, NJ (2007).
36. M.J. Cleare and W.P. Griffith, *J. Chem. Soc. A*, 1144 (1967); https://doi.org/10.1039/j19670001144
37. A.B.P. Lever, Inorganic Electronic Spectroscopy, Elsevier: Amsterdam (1986)
38. F.B. Biswas, T.G. Roy, M.A. Rahman and T.B. Emran, *Asian Pac. J. Trop. Med.*, **7**, S534 (2014); https://doi.org/10.1016/S1995-7645(14)60286-8